A network model of channel competition in fracture dissolution

P. Szymczak[1] and A. J. C. Ladd[2]

Received 28 November 2005; revised 19 January 2006; accepted 24 January 2006; published 1 March 2006.

[1] During dissolution in porous or fractured rock, a positive feedback between fluid transport and chemical reactions at the mineral surfaces may lead to the formation of pronounced, wormhole-like channels. As the dissolution proceeds the channels interact, competing for the available flow, and eventually the growth of the shorter ones ceases. Thus the number of channels decreases with time while the characteristic distance between them increases, which leads to a scale-invariant, power-law distribution of channel lengths. A simple resistor network model of the evolution of dissolving channels is constructed and its properties studied. The results are compared with pore-scale simulations of fracture dissolution using a microscopic, three-dimensional numerical model. Despite its simplicity, the resistor model is found to retain the essential features of the nonlinear interaction between the channels. **Citation:** Szymczak, P., and A. J. C. Ladd (2006), A network model of channel competition in fracture dissolution, *Geophys. Res. Lett.*, *33*, L05401, doi:10.1029/2005GL025334.

1. Introduction

[2] The coupling between fluid flow and chemical kinetics is a key element to developing a quantitative or even a qualitative understanding of important geological processes. One manifestation of this coupling is the development of channels during dissolution of fractured or porous rock. These channels become a means for very rapid transport within the rock matrix and play an important role in fundamental and applied geophysical problems, such as the development of limestone caverns or the sequestration of CO_2. It has long been known [*Ortoleva et al.*, 1987] that a planar dissolution front propagating through a homogeneous porous matrix is unstable with respect to small variations in local permeability; regions of high permeability dissolve faster because of enhanced transport of reactants, which leads to increased rippling of the front.

[3] In this letter we concentrate on the next stage of the system evolution, when nonlinear interactions between finite-amplitude perturbations to the front cause the dissolution pattern to change qualitatively. Experiments [*Detwiler et al.*, 2003] and simulations [*Cheung and Rajaram*, 2002; *Szymczak and Ladd*, 2004b] have shown that under certain flow conditions the initially sinusoidal instability grows into pronounced channels which advance ahead of the front. Next, as the dissolution proceeds, the channels interact and compete for flow [*Hoefner and Fogler*, 1988]. As a result, the flux in the larger channels increases whereas the smaller ones cease to grow and finally disappear as the dissolution front advances. This leads to a new dissolution pattern which is characterized by a length scale different from the wavelength of the initial instability.

[1]Institute of Theoretical Physics, Warsaw University, Warsaw, Poland.
[2]Chemical Engineering Department, University of Florida, Gainesville, Florida, USA.

0094-8276/06/2005GL025334$05.00

2. Pore Scale Simulations

[4] To investigate channel growth and interaction in a dissolving fracture, we use a recently developed pore-scale numerical model [*Szymczak and Ladd*, 2004b]. In the model, the velocity field in the pore space is calculated by an implicit lattice-Boltzmann technique [*Verberg and Ladd*, 1999] while the transport of dissolved species is modeled by a random walk algorithm that efficiently incorporates the chemical kinetics at the solid surfaces [*Szymczak and Ladd*, 2004a]. The fracture surfaces are divided into pixels (for the results reported below 800×800 pixels were used) and the height of each pixel is eroded in response to contacts by tracer particles. The time evolution of the velocity field and local aperture field in the fracture are determined by iterating this procedure, removing small amounts of material at each step and calculating the reactant distribution and flow field for the updated topography. The simulation method has been validated by comparison with experimental data on an identical initial topography [*Szymczak and Ladd*, 2004b].

[5] This time, the model was applied to simulate dissolution in fractures with numerically generated topographies. The fracture surfaces are initially flat and the space between them is filled with several thousand randomly placed cubes ($3 \times 3 \times 3$ pixels), which span the gap between the surfaces. The reactive fluid enters from one side (left side of Figure 1) and exits from the other, while no-slip boundaries are assumed on the other faces of the fracture. Thus both the setup and the initial fracture topography resemble that analyzed experimentally by *Detwiler et al.* [2003]. The protrusions are initially placed at the vertices of a square centered lattice with a separation of one pixel between them and then randomly shifted by one pixel along the lateral direction (perpendicular to the fluid flow). Such a procedure guarantees that the fluid can percolate through the fracture, and generates a short-range spatial correlation length with no discernable long-range structure. Thus we could be sure that the dissolution channels appear spontaneously and are not determined by any pre-existing channels. In contrast, variable aperture fractures often show strong channeling even in the absence of the dissolution [e.g., *Johns and Roberts*, 1991, and references therein]. Analysis of dissolution-induced phenomena in such systems is harder than the present case, and will be the subject of a future publication.

[6] A constant pressure difference was applied across the ends of the fracture, to generate flows corresponding to initial values of the Peclet number, $Pe = Uh_0/D$, of 1 and 8 respectively. Here U is a characteristic fluid velocity, h_0 is the initial mean aperture and D is the solute diffusion coefficient. The dissolution at the fracture surfaces was assumed to be instantaneous, corresponding to a zero reactant concentration at the fluid-rock interfaces. A transport limited case was chosen not just because of its simplicity, but also because a number of preparatory simulations, performed for a wide range of fluid flow and

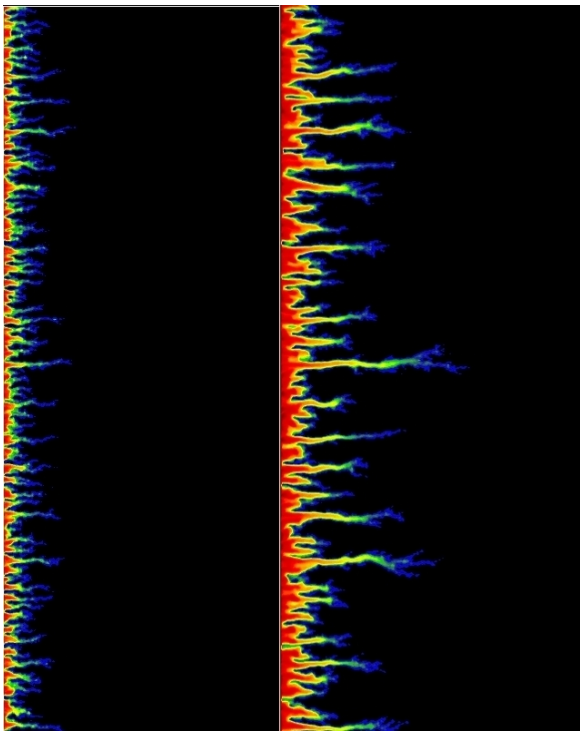

Figure 1. Aperture growth due to dissolution in an artificial fracture at $Pe = 8$. The figure shows dissolution patterns at (left) $\Delta h = 0.15h_0$ and (right) $\Delta h = 0.5h_0$. The colors indicate regions of low (blue), medium (green), and high (red) aperture growth. The flow direction is from left to right. Only 1/3 of the fracture (the leftmost part) is shown.

reaction rates, have shown that channeling is most pronounced at high reaction rates and moderate Peclet numbers. Simulations were carried out up to the point when the total fluid volume inside the fracture increased approximately twofold; that is, $\Delta h \sim h_0$, with Δh being the difference between the final and initial aperture.

[7] A typical result of the simulation is shown in Figure 1, where the dissolution patterns are captured at two different times, corresponding to $\Delta h = 0.15h_0$ and $0.5h_0$ respectively. Only a small fraction of the channels present at $\Delta h = 0.15h_0$ persist to later times ($\Delta h = 0.5h_0$); the channels that do survive have advanced considerably ahead of the dissolution front. As a result, the characteristic length between active (growing) channels is increasing. If the simulation is run longer, the process repeats itself, leaving only a few active channels in the sample at the end. To analyze the phenomenon more precisely, we consider the distribution of channel length. The quantity of interest is $N(L, t)$, the number of channels longer than L at time t. The linear fit

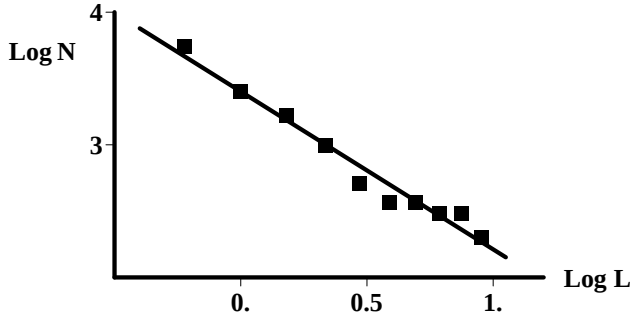

Figure 2. The cumulative distribution $N(L)$ of channel lengths in the fracture simulated with the pore scale model ($Pe = 8$). The solid line has a slope of -1.2 and all logarithms are natural.

in the log-log plot, shown in Figure 2, indicates a power law decay,

$$N(L) \sim L^{-m}, \tag{1}$$

where the exponent m is equal to 1.2 ± 0.15 for $Pe = 8$ and 1.4 ± 0.2 for $Pe = 1$. Interestingly, these exponents are close to those reported for the distribution of lengths of viscous fingers in a Hele-Shaw cell [*Roy et al.*, 1999]. The data depicted in Figure 2 corresponds to the dissolution pattern at $\Delta h = 0.5h_0$ (cf. the right pattern in Figure 1) but the same scaling and exponent are observed over a wide time range, corresponding to a change in aperture between $\Delta h \approx 0.3h_0$ and $\Delta h = h_0$.

[8] The log-periodic oscillations in $N(L)$, clearly visible in Figure 2, as well as in the analogous data for $Pe = 1$ case, are a signature of discrete scale invariance (DSI). Unlike continuous scale invariance, where self-similarity is characterized by an invariance with respect to arbitrary magnifying factors, a DSI system is invariant under a discrete set of dilatations only. Discrete scale invariance has been observed in distributions of joints formed under thermal stress, in diffusion limited aggregation systems and in viscous fingering patterns [see *Huang et al.*, 1997; *Sornette*, 1998; *Roy et al.*, 1999, and references therein].

3. The Model

[9] The power-law scaling shown in Figure 2 suggests a simple mechanism underlying the phenomenon of channel selection, which may be revealed if all inessential details are eliminated. Specifically, we hypothesize that the core of the interaction between the channels is the capture of flow from shorter channels by longer ones. In fact, it was established experimentally [*Kelemen et al.*, 1995] that the flow lines in the vicinity of a dissolving channel are converging near its inlet and diverging at its outlet, as shown schematically in Figure 3. This can be elucidated by looking at the pressure drops in the channels, depicted schematically in the bottom plot of Figure 3. For simplicity, we assume here that the channels are of a constant aperture. Since there is a constant pressure drop between the inlet and outlet, the pressure gradient in the longer channel will be steeper than in the shorter channel; this is because the flow rate is higher in the long channel. In the upstream part of the fracture the short

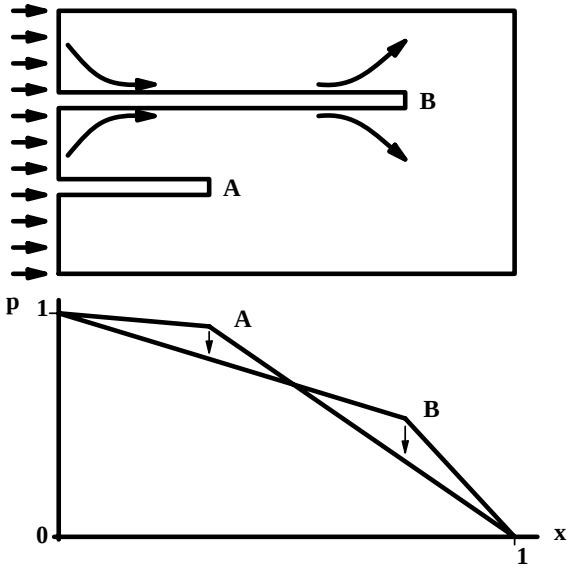

Figure 3. Two dissolution channels in the fracture (top) and the corresponding pressure drops (bottom). The flow lines are converging toward a larger channel at the inlet and diverging near the tip of the conduit.

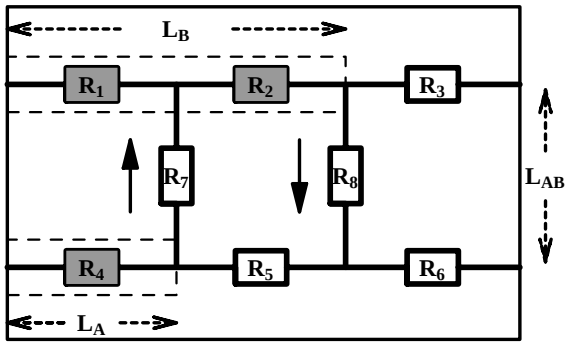

Figure 4. A resistor network corresponding to the configuration of Figure 3. The arrows denote the directions of the currents between the channels.

channel is at a higher pressure than the long one, so flow is directed toward the long channel. Downstream, the region around the tip of the long channel is at a higher pressure than the surrounding medium and so flow is directed away from the channel, resulting in the flow pattern seen in the experiments [*Kelemen et al.*, 1995]. Note that the larger the difference in channel lengths, the higher the pressure drop between the channels. Since the larger flow in the channel leads to increased dissolution, this generates the positive feedback loop resulting in fast growth of the longer channels and starvation of the shorter ones.

[10] We propose the following simplified model of channel-channel interactions, which retains the flow capturing mechanism described above. In the model, the fracture is represented as a resistor network with two types of resistors: low resistance (C), representing the channels, and high resistance (M), representing the undissolved medium. For example, the two-channel system in Figure 3 can be represented by eight resistors, as shown in Figure 4. To keep the model simple, we assume that the resistance is simply a product of the resistor length and a resistivity, which is taken to be constant for both C and M resistors. Thus, for the configuration in Figure 4

$$R_1 = R_4 = \rho_C L_A, \qquad R_2 = \rho_C (L_B - L_A),$$
$$R_3 = R_6 = \rho_M (L_{tot} - L_B), \quad R_5 = \rho_M (L_B - L_A), \tag{2}$$
$$R_7 = R_8 = \rho_M L_{AB},$$

where L_B and L_A are the lengths of the respective channels (cf. Figure 3), L_{tot} is the total length of the fracture and L_{AB} is the distance between the channels. The resistivities (resistance per unit length) are denoted by ρ_C and ρ_M. Next, given the constant potential difference between the edges (which corresponds to the constant pressure drop across the fracture), all the respective currents $I_1 \ldots I_8$ can be calculated by straightforward algebra. In particular, it is possible to show that, if $L_B > L_A$, then the lateral currents between the conduits (I_7 and I_8) are directed as shown in Figure 4. Thus the flow is indeed being sucked out of the shorter channels by the nearby longer ones.

[11] Finally, a dissolution dynamics for the system must be defined. Here we assume a simple rule that the increase in the length of the channel is proportional to the current at its tip, that is, for the configuration shown in Figure 4

$$\frac{dL_B}{dt} = I_2, \qquad \frac{dL_A}{dt} = I_4. \tag{3}$$

This corresponds to the assumption that the Peclet number is sufficiently high that an increase in the length of the channel is much larger than the change in its lateral dimensions. The limitation that the channels only grow at the tip makes our model similar to needle models of growth in diffusion-limited aggregation [*Krug*, 2002]. However, the dynamics defined by equations (2) and (3) are quite different from the Laplacian growth of diffusion-limited aggregation.

[12] Let us now consider the situation at the early stages of the dissolution process, when the lengths of the channels are relatively small compared to the length of the sample, L_A, $L_B \ll L_{tot}$. This condition, together with the condition that the dissolved region has a much higher permeability than the undissolved medium, $\rho_C/\rho_M \ll 1$, implies that

$$R_3, R_6 \gg R_7, R_8, R_5 \gg R_1, R_2, R_4. \tag{4}$$

In this limit, the ratio of the currents in both channels, which according to equation (3) determines their evolution, is simply

$$\frac{\dot{L}_B}{\dot{L}_A} = \frac{I_4}{I_2} = 1 + \frac{2R_5}{R_7} = 1 + \frac{2(L_B - L_A)}{L_{AB}}. \tag{5}$$

This result agrees with the qualitative observation of *Hoefner and Fogler* [1988] that the ratio of the difference in the lengths of the channels to the distance between them is the quantity governing the evolution of the dissolving conduits.

[13] Next, we generalize the model to the N-channel case. As before, we connect the tip of each channel with every other channel to allow for redistribution of the flow. This defines a network of $2N^2$ resistors. The dissolution dynamics is obtained analogously to equation (3),

$$\frac{dL_i}{dt} = I_i, \qquad i = 1, \ldots \tag{6}$$

where I_i is the current at the tip of i–th resistor. Again, the currents for the given set of resistances may be obtained by the linear solver and then the dynamics is iterated to track the evolution of the system.

4. Results

[14] A typical result obtained with use of the above rules is shown in Figure 5. Here, 1200 channels are simulated

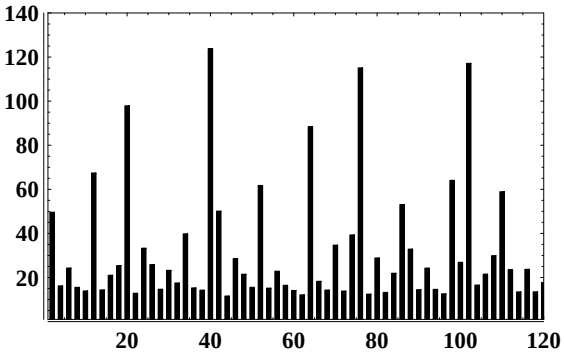

Figure 5. Map of the channels grown according to the resistor network rules. The figure shows 1/10 of the width of the simulated system.

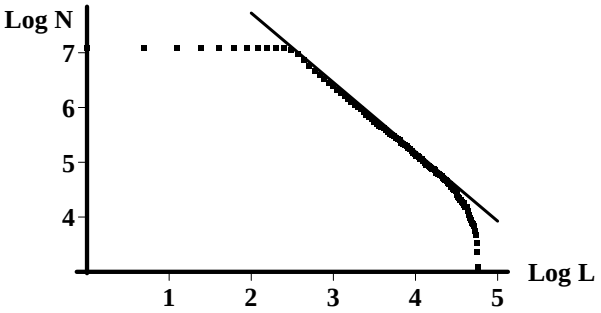

Figure 6. The cumulative distribution $N(L)$ of channel lengths from in the fracture simulated with the resistor network model. The solid line has a slope of −1.25.

with the initial length chosen uniformly at random from the interval [6,10]. The spacing between the neighboring channels is constant and equal to 1 whereas the total length of the sample L_{tot} = 1500. Finally, the resistivities are $\rho_C = 1$ and $\rho_M = 20$ respectively. To avoid finite-size effects, the computation was continued until the longest channel reached 1/10 of the length of the sample.

[15] Figure 6 shows the cumulative distribution of channel lengths for the simulated system. We find a power-law decay over a wide range of L, with an exponent equal to m = 1.25, in very good agreement with the pore-scale simulations. Moreover, the value of the exponent turns out to be insensitive to the details of the simulation, such as the initial distribution of channel length, channel spacing or even the values of the resistivities as long as their ratio, ρ_C/ρ_M, remains small. This suggests that the value of m may be universal.

[16] The log-periodic oscillations observed in the pore-scale simulations are absent from the data obtained from the network model (Figure 6). This is due to the random dephasing between channels in distant parts of the sample [*Sornette*, 1998]. Indeed, in the early stages of the dissolution recent numerical simulations [*Szymczak and Ladd*, 2004b] found very limited interaction between different areas of the fracture. The dissolution pattern at a cross-stream location y_0 depends only on the topography in its immediate neighborhood $|y - y_0| < d$, where d is the interaction range. Although the interaction range increases as the dissolution channels develop, still the distant parts of the sample evolve essentially independently of each other. Thus the process of self-averaging takes place, which destroys the logarithmic oscillations [*Sornette*, 1998]. In the pore-scale simulations, self averaging is absent because of the small sample size (only ∼60 channels compared to 1500 in the network model). In fact, if we limit the sample size in the network model and average $N(L)$ over only one hundred neighboring channels, the log-periodic oscillations in $N(L)$ appear once again.

[17] Naturally, the model we have described only captures some aspects of the fracture evolution. One feature that is not taken into account is tip splitting, which plays an important role in fractures of high aperture variability [*Cheung and Rajaram*, 2002]. However, even in fractures of smaller variability, tip splitting become very pronounced as the channel tip nears the outlet. Thus, strictly speaking, our model is applicable to the intermediate stages of fracture dissolution, when on one hand the channels have grown considerably from the initial ripples but on the other hand they are relatively short in comparison with the length of the fracture. In principle it would be possible to include the effects of tip splitting into the resistor network model, by allowing the vertical resistances, like R_7 and R_8 (Figure 4), to dissolve as well. However this would make the model significantly more complex.

5. Summary

[18] In this paper we have studied channel growth and competition in a dissolving porous medium. The dissolution patterns obtained with use of the pore-scale numerical model have shown scale-invariant properties. A model of interaction between flow channels was constructed, by mapping the system into an evolving resistor network. Although simple, the model retains the crucial flow capturing mechanism, which causes a fast growth of longer channels and starvation of the shorter ones. The network model shows the same nontrivial scaling features as the dissolving fracture system, which confirms the hypothesis that the flow-capturing mechanism is indeed one of the main driving factors in channel evolution.

[19] **Acknowledgments.** The lattice-Boltzmann code used in the pore-scale simulations was written by Rolf Verberg (University of Pittsburgh). This work was supported by the Polish Committee of Scientific Research (P03B 08127, 2004–2005), and by the U.S. Department of Energy, Chemical Sciences, Geosciences and Biosciences Division, Office of Basic Energy Sciences (DE-FG02-98ER14853).

References

Cheung, W., and H. Rajaram (2002), Dissolution finger growth in variable aperture fractures: Role of the tip-region flow field, *Geophys. Res. Lett.*, *29*(22), 2075, doi:10.1029/2002GL015196.

Detwiler, R. L., R. J. Glass, and W. L. Bourcier (2003), Experimental observations of fracture dissolution: The role of Peclet number in evolving aperture variability, *Geophys. Res. Lett.*, *30*(12), 1648, doi:10.1029/2003GL017396.

Hoefner, M., and H. Fogler (1988), Pore evolution and channel formation during flow and reaction in porous media, *AIChE J.*, *34*, 45–54.

Huang, Y., G. Ouillon, H. Saleur, and D. Sornette (1997), Spontaneous generation of discrete scale invariance, *Phys. Rev. E*, *55*, 6433–6447.

Johns, R. A., and P. V. Roberts (1991), A solute transport model for channelized flow in a fracture, *Water Resour. Res.*, *27*, 1797–1808.

Kelemen, P. B., A. Whitehead, E. Aharonov, and K. A. Jordahl (1995), Experiments on flow focusing in soluble porous media, with applications to melt extractions from the mantle, *J. Geophys. Res.*, *100*(B1), 475–496.

Krug, J. (2002), Origin of scale invariance in growth processes, *Adv. Phys.*, *46*, 139–282.

Ortoleva, P., J. Chadam, E. Merino, and A. Sen (1987), Geochemical self-organisation II: The reactive-infiltration instability, *Am. J. Sci.*, *287*, 1008–1040.

Roy, A., S. Roy, A. J. Bhattacharayya, S. Banarjee, and S. Tarafdar (1999), Discrete scale invariance in viscous fingering patterns, *Eur. Phys. J. B*, *12*, 1–3.

Sornette, D. (1998), Discrete scale invariance and complex dimensions, *Phys. Rep.*, *297*, 239–270.

Szymczak, P., and A. J. C. Ladd (2004a), Stochastic boundary conditions to the convection-diffusion equation including chemical reactions at solid surfaces, *Phys. Rev. E.*, *69*, 036704.

Szymczak, P., and A. J. C. Ladd (2004b), Microscopic simulations of fracture dissolution, *Geophys. Res. Lett.*, *31*, L23606, doi:10.1029/2004GL021297.

Verberg, R., and A. J. C. Ladd (1999), Simulation of low-Reynolds-number flow via a time-independent lattice-Boltzmann method, *Phys. Rev. E*, *60*, 3366–3373.

A. J. C. Ladd, Chemical Engineering Department, University of Florida, Gainesville, FL 32611-6005, USA.

P. Szymczak, Institute of Theoretical Physics, Warsaw University, Hoża 69, 00-618, Warsaw, Poland. (piotrek@fuw.edu.pl)